Study of Isomer Production Rates for A=142-152 and Z=62-67 in Fragmentation of a Relativistic 208Pb Beam

Myalski, S.; Maj, A.; Podolyak, Zs.; Kmiecik, M.; Bednarczyk, P.; Grebosz, J.; Regan, P. H.; Garnsworthy, A. B.; Pietri, S.; Rudolph, Dirk; Steer, S. J.; Becker, F.; Gerl, J.; Gorska, M.; Grawe, H.; Kojouharov, I.; Schaffner, H.; Wollersheim, H. J.; Prokopowicz, W.; Benzoni, G.; Blank, B.; Brandau, C.; Bruce, A. M.; Caceres, L.; Camera, F.; Catford, W. N.; Cullen, I. J.; Dombradi, Zs.; Doornenbal, P.; Estevez, E.; Geissel, H.; Gelletly, W.; Heinz, A.; Hoischen, Robert; Ilie, G.; Jones, G. A.; Jungclaus, A.; Kelic, A.; Kondev, F. G.; Kurtukian-Nieto, T.; Kurz, N.; Lalkovski, S.; Liu, Z.; Montes, F.; Pfuetzner, M.; Saito, T.; Shizuma, T.; Simons, A. J.; Schwertel, S.; Tachenov, S.

Published in:
Acta Physica Polonica. Series B: Elementary Particle Physics, Nuclear Physics, Statistical Physics, Theory of Relativity, Field Theory

DOI:
10.5506/APhysPolB.43.253

2012

LUND UNIVERSITY

PO Box 117
221 00 Lund
+46 46-222 00 00

STUDY OF ISOMER PRODUCTION RATES FOR $A = 142$–152 AND $Z = 62$–67 IN FRAGMENTATION OF A RELATIVISTIC ^{208}Pb BEAM*

S. Myalski[a], A. Maj[a], Zs. Podolyák[b], M. Kmiecik[a], P. Bednarczyk[a] J. Grębosz[a,c], P.H. Regan[b], A.B. Garnsworthy[b,d], S. Pietri[b], D. Rudolph[e] S.J. Steer[b], F. Becker[c], J. Gerl[c], M. Górska[c], H. Grawe[c], I. Kojouharov[c] H. Schaffner[c], H.J. Wollersheim[c], W. Prokopowicz[c,f], G. Benzoni[g] B. Blank[i], C. Brandau[b], A.M. Bruce[j], L. Cáceres[e,k], F. Camera[h] W.N. Catford[b], I.J. Cullen[b], Zs. Dombradi[l], P. Doornenbal[c], E. Estevez[m] H. Geissel[c], W. Gelletly[b], A. Heinz[n], R. Hoischen[e], G. Ilie[n,o], G.A. Jones[b] A. Jungclaus[k], A. Kelic[c], F.G. Kondev[p], T. Kurtukian-Nieto[m], N. Kurz[c] S. Lalkovski[r], Z. Liu[b], F. Montes[e], M. Pfützner[s], T. Saito[c], T. Shizuma[b,t] A.J. Simons[b], S. Schwertel[u], S. Tachenov[c], P.M. Walker[b] E. Werner-Malento[c,s], O. Wieland[g]

[a]Institute of Nuclear Physics, Polish Academy of Sciences, 31-342, Kraków, Poland
[b]Department of Physics, University of Surrey, Guildford, GU2 7XH, UK
[c]GSI, Planckstrasse 1, 64291 Darmstadt, Germany
[d]WNSL, Yale University, 272 Whitney Avenue, New Haven, CT, 06520, USA
[e]Department of Physics, Lund University, 22100 Lund, Sweden
[f]Institute of Physics, Jagiellonian University, 30-059 Kraków, Poland
[g]INFN sez. di Milano, Via Celoria 16, 20133 Milano, Italy
[h]Universita' degli Studi di Milano and INFN sez. Milano, 20133 Milano, Italy
[i]CENBG, le Haut Vigneau, 33175 Gradignan Cedex, France
[j]School of Engineering, University of Brighton, Brighton, BN2 4GJ, UK
[k]Departamento de Fisica Teorica, Universidad Autonoma de Madrid, 28049 Madrid, Spain
[l]Institute for Nuclear Research, 4001 Debrecen, Hungary
[m]Universidad de Santiago de Compostela, 15706 Santiago de Compostela, Spain
[n]IKP, Universität zu Köln, 50937 Köln, Germany
[o]National Institute of Physics and Nuclear Engineering, Bucharest, Romania
[p]Nuclear Engineering Division, ANL, Argonne, IL-60439, USA
[r]Faculty of Physics, University of Sofia "St. Kliment Ohridsk" Sofia, Bulgaria
[s]Faculty of Physics, University of Warsaw, Hoża 69, 00-681 Warszawa, Poland
[t]Japan Atomic Energy Research Institute, Kyoto, 619-0215, Japan
[u]Physik Department E12, Technische Universitat München, Garching, Germany

(Received November 14, 2011)

We have investigated nuclear fragmentation reactions of a relativistic ^{208}Pb beam. Ten isomeric states for nuclei with $A = 142$–152 and $Z = 62$–67 were observed. Measured isomeric ratios were compared, together with values from other experiments, with prediction of theoretical models. The discrepancies between the experimental and theoretical values were discussed in terms of transitions by-passing the isomer that are not included in the models.

DOI:10.5506/APhysPolB.43.253
PACS numbers: 29.30.Kv, 25.75.–q, 23.35.+g, 25.70.Mn

* Presented at the XXXII Mazurian Lakes Conference on Physics, Piaski, Poland, September 11–18, 2011.

1. Introduction

The production of isomeric states in the fragmentation of a relativistic (1 GeV/u) ^{208}Pb beam on ^{9}Be target (2.526 g/cm^3 thick) was investigated. Fragments selected by the fragment separator FRS at GSI [1], Germany, were implanted in a stopper positioned in the FRS focal plane. Only fragments of A = 140–160 and Z = 60–70 were delivered to the RISING setup at the final focal plane of the fragment separator. γ rays from the decay of isomeric states in the nuclei were detected with the high purity germanium array of RISING [2,3]. Isomeric ratios (the fraction of nuclei in the isomeric state) were extracted for ten isomeric states: 19^- in ^{152}Ho, $31/2^+$ in ^{153}Ho, 27^+ in ^{148}Tb, 10^+ in ^{144}Gd, $49/2^+$ in ^{147}Gd, $11/2^-$ in ^{143}Eu, 8^- in ^{144}Eu, $11/2^-$ in ^{145}Eu, 10^+ in ^{142}Sm and 7^- in ^{142}Sm, with half-lives ranging from 145 nanoseconds to 50 microseconds. The extracted isomeric ratios (IR), together with the results from other experiments, are summarized in Tables I and II. Details of the data analysis have been described in references [4,5].

TABLE I

Comparison of observed and calculated isomeric ratios for ^{238}U beam. Detailed description in the text.

Nucleus	Spin	yrast	IR_{exp}	IR_{form}	IR_{ABR}	IR_{INC}	σ_f	Cite
^{195}Pb	$\frac{21}{2}$-	N	15±2.8	48.4	40.7	88.3	8.3	[6]
^{196}Pb	5-	T	50±4	83.2	71.5	83.7	8.2	[6]
^{192}Tl	8-	T	22±10	66.6	56.9	95.6	8.6	[6]
^{202}Po	8+	T	4.5±1.2	60	49.8	92.9	7.7	[6]
^{188}Hg	12+	T	6.2±1.9	44.3	34.1	85.3	8.9	[6]
^{200}Po	11-	T	39.3±1.2	41	27.5	76.7	7.9	[6]
^{192}Pb	12+	T	14±3	41.5	28.2	82.8	8.6	[6]
^{194}Pb	12+	T	16±4	40	28	82.9	8.4	[6]
^{196}Pb	12+	T	17±30	38.4	27.8	97.1	8.2	[6]
^{198}Po	12+	T	8.9±1.2	36.7	20	72.4	8	[6]
^{200}Po	12+	T	6.7±4.1	34.9	22.2	73.3	7.9	[6]
^{195}Bi	$\frac{29}{2}$-	T	4.5±0.9	25.9	15.3	56.6	8.3	[6]
^{197}Bi	$\frac{29}{2}$-	T	8±2	24.4	16.5	61.5	8.1	[6]
^{193}Pb	$\frac{33}{2}$+	T	1.5±0.4	19	11.3	59.3	8.5	[6]
^{206}Pb	7 -	N	52±8	63	58	94	7.2	[7]
^{206}Pb	12 +	N	29±5	27.6	25	79	7.2	[7]
^{203}Tl	($\frac{25}{2}$.$\frac{29}{2}$) +	T	21±4	23	25	78	7.6	[7]
^{205}Tl	$\frac{25}{2}$ +	T	25±5	25.9	23	77	7.3	[7]
^{205}Pb	$\frac{25}{2}$ -	T	29±5	25.9	23	76	7.3	[7]
^{211}Bi	$\frac{25}{2}$ -	T	17±7	19.4	17	86	6.7	[7]
^{204}Tl	20 +	T	9±3	3.8	3	81	7.4	[7]

TABLE II

Comparison of observed and calculated isomeric ratios for ^{208}Pb beam. Detailed description in the text.

Nucleus	Spin	yrast	IR_{exp}	IR_{form}	IR_{ABR}	IR_{INC}	σ_f	Cite
^{142}Sm	10+	N	2±0.9	59.8	75.5	87.9	10.4	[5]
^{143}Eu	$\frac{11}{2}$-	T	13.1±2.8	88.9	91.3	97.4	10.4	[5]
^{145}Eu	$\frac{11}{2}$-	T	25.9±4.1	88.7	90.7	96.1	10.2	[5]
^{142}Sm	7-	T	29.9±6.75	82.2	87	95.7	10.4	[5]
^{144}Eu	8-	T	15.6±2.2	76.4	82.7	94.1	10.3	[5]
^{144}Gd	10+	T	12.3±5.6	59	75.2	87.2	10.3	[5]
^{153}Ho	$\frac{31}{2}$+	T	21.4±6.5	24.5	15.3	75.7	9.6	[5]
^{152}Ho	19-	T	6±2	15.7	32.4	49.8	9.7	[5]
^{147}Gd	$\frac{49}{2}$+	T	1.9±0.9	4.4	18.2	27.9	10.1	[5]
^{148}Tb	27+	T	1.9±0.3	2.1	12.4	19.7	10	[5]
^{177}Ta	$\frac{5}{2}$ -	N	4±0.6	92.1	91	99.3	7.4	[8]
^{136}Sm	8 -	N	3.5±1.2	73.2	70.2	91.5	10.8	[8]
^{138}Gd	8 -	N	5±1	72.7	69.3	91.4	10.7	[8]
^{176}Hf	6 +	N	6±2	68.3	64.4	97.8	7.5	[8]
^{174}Hf	8 -	N	2±0.5	53.9	49.3	94.9	7.7	[8]
^{175}Hf	$\frac{19}{2}$ +	N	3±1	41.5	36.5	92.9	7.6	[8]
^{175}Ta	$\frac{21}{2}$ +	N	2±0.5	34.5	29.5	80.4	7.6	[8]
^{177}Ta	$\frac{21}{2}$ -	N	9±2	32.3	27.1	85.8	7.4	[8]
^{179}W	$\frac{21}{2}$ +	N	6±1	30	25.7	87.5	7.1	[8]
^{181}W	$\frac{21}{2}$ +	N	17±4	27.6	23.6	88.2	6.9	[8]
^{181}Re	$\frac{25}{2}$ +	N	2.8±0.5	16.5	13.1	80.7	6.9	[8]
^{185}Re	$\frac{21}{2}$ -	N	21±6	22.2	18.6	79.6	6.4	[8]
^{176}Ta	14 -	N	2.6±0.5	14.8	11	70.3	7.5	[8]
^{180}W	14 -	N	6.4±1	11.5	8.9	81.6	7	[8]
^{179}W	$\frac{35}{2}$ -	N	2.7±0.5	4	2.4	67.2	7.1	[8]
^{181}Re	$\frac{35}{2}$ -	N	0.2±0.1	3.15	2	60.8	6.9	[8]
^{181}W	$\frac{5}{2}$ -	T	6±1	91.1	90.1	99.6	6.9	[8]
^{206}Hg	5 -	T	3.7±0.7	1.58	32.5	92.8	1.9	[8]
^{182}W	10 +	T	10±2	29.6	25.6	89.9	6.8	[8]
^{200}Pt	7 -	T	30±5	14.2	35.5	88.6	3.8	[8]
^{179}Ta	$\frac{21}{2}$ -	T	9±3	30	24.9	88.2	7.1	[8]
^{180}Ta	15 -	T	10±3	8.4	6.1	77	7	[8]
^{175}Hf	$\frac{35}{2}$ -	T	2.5±0.6	5.8	3.8	66.6	7.6	[8]
^{203}Hg	$\frac{13}{2}$ +	T	12±2	6.7	24.7	88.9	3	[9]
^{203}Au	$\frac{11}{2}$ -	T	3±1	13.7	48.5	94.6	3	[9]

2. Theoretical predictions of fragment spin

Calculations of angular momentum distributions were made to reproduce experimental conditions, using three theoretical models: an analytical formula, which takes into account only the projectile and fragment nucleon properties [10]; a macroscopic, geometrical approach — Abrabla code [11]; and a microscopic, nucleon–nucleon collision code — IntraNuclear Cascade [12] coupled to the GEMINI++ evaporation code [13]. Each model was used to calculate the angular momentum distribution of final fragments produced in the fragmentation of ^{208}Pb beam. The results are shown in Fig. 1.

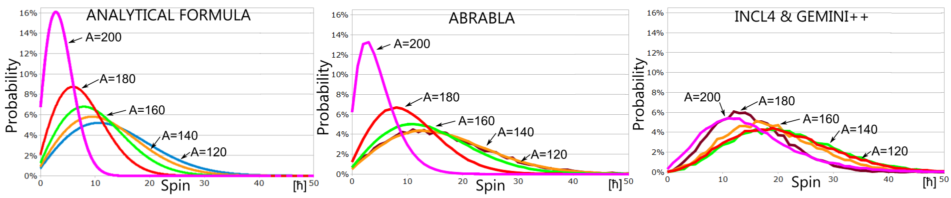

Fig. 1. Calculated spin distribution for the fragmentation of ^{208}Pb beam at 1 GeV/u on ^{9}Be target, for different fragment mass.

As the models only provide information about the spin distribution of entry states (before γ de-excitation starts), the sharp cut-off approach was used to calculate the isomeric ratios. Its two main assumptions are: all fragments produced with higher spin than that of the isomeric state will de-excite to the isomeric state and there are no transitions by-passing the isomeric state. In reality, these assumptions are almost always violated which leads to the overestimation of the isomeric ratios by the models. Such an approach, providing that the model gives a realistic spin distribution of fragments, may give only the upper limit of the isomeric ratio.

3. Comparison of theoretical and experimental isomeric ratios

For more detailed comparison between experimental and theoretical isomeric ratios, additional data from other relativistic fragmentation experiments (using the RISING setup) were used, and they are shown in Tables I and II. "Spin" column gives the spin of the isomeric state, "yrast" tells us whether this is an yrast isomer (Y — Yes, N — No), IR_{exp}, IR_{form}, IR_{ABR}, IR_{INC} are isomeric ratios observed in experiment, and calculated using the analytical formula, Abrabla model, and INC+Gemini++ model respectively. According to the analytical formula, the isomeric ratio for an isomer of spin I is given by [8]

$$\mathrm{IR_{form}} = \exp\left[-\frac{I(I+1)}{2\sigma_f^2}\right] , \tag{1}$$

where σ_f is the spin cut-off parameter, which depends on fragment (A_f) and projectile (A_p) mass

$$\sigma_f^2 = \langle j_z^2 \rangle \frac{(A_\mathrm{f} + \nu A_\mathrm{p})(A_\mathrm{p} - A_\mathrm{f})}{(A_\mathrm{p} - 1)(\nu + 1)^2} , \tag{2}$$

ν is the ratio of evaporated to abraded nucleons ($\nu = 2$ [10]), and $\langle j_z^2 \rangle$ is the average square of the angular momentum projection of a nucleon.

A comparison of the theoretical models shows that ABRABLA predicts on average values of isomeric ratios closest to those observed, and using the analytical formula we get similar values to ABRABLA. In contrast, the IntraNuclear Cascade code coupled to GEMINI++ produced much higher estimates of isomeric ratio values. In addition, the spin distributions calculated with this model extend to much higher spins. We conclude that the INTRANUCLEAR CASCADE with GEMINI++, at the present stage of its development and for heavy projectile and fragment, does not seem to reproduce properly the spin distributions of the fragments. It seems to be evident from an examination of Tables I and II that the experimental IR values for isomers denoted as non-yrast are very small and much smaller than the predictions of the models. Similarly it seems that isomers with lower spin have smaller values of isomeric ratio, comparing to the theoretical predictions. To quantify this supposition in a more general statistical way, Table III was created, where the average ratio of the experimental isomeric ratio to the theoretical one was computed, after grouping the results of Tables I and II into 4 classes, depending on whether the isomer is yrast or non-yrast, and whether its spin is higher or lower than the spin cut-off parameter σ_f. Only

TABLE III

Average percentage of predicted isomeric ratio value actually observed in experiment. Results are divided into yrast ($T = 0$), non-yrast isomers ($T > 0$) and with spin above σ_f and below σ_f. "Events" column shows the number of isomeric states from Tables I and II which satisfy the criteria.

	ABRABLA	Analytical formula	Events
$> \sigma_f$, $T = 0$	67%	75%	28
$< \sigma_f$, $T = 0$	28%	28%	8
$> \sigma_f$, $T > 0$	47%	37%	14
$< \sigma_f$, $T > 0$	20%	18%	6

the analytical formula and Abrabla model were used for comparison. Providing that the angular distribution of the fragments is calculated properly, the values in Table III tell us the fraction of the γ-flow from the spins higher than the isomer that pass through the isomeric state. For discussion of the results, one can use the schematic drawing depicting the de-excitation of the fragment's entry region (Fig. 2). For the non-yrast, low spin isomers only a few decay paths may "hit", therefore the experimental isomeric ratio can be low — the transition can by-pass this isomer not only by proceeding through the yrast line, but also by many other paths. Indeed. in the table we find a value of *ca.* 20%, hence *ca.* 80% of the γ-flow by-passes such isomer. For high spin yrast isomers the situation is different. Many γ-paths in the flux reach the yrast line and feed the isomeric state. However, there are still some transitions that proceed via excited bands, parallel to the yrast line, by-passing the isomer. Indeed, the table for such a case shows that *ca.* 70% of the flow passes through the isomeric state. For yrast isomers at lower spins, the statistical cascades are longer, so there are more chances to by-pass the isomer — from the table we can find a value of *ca.* 30% of the γ-flow pass through such isomers. This simple consideration explains in a qualitative way the results in Table III. In order to make the quantitative predictions for the isomeric ratios, one has to improve the theoretical models, such as Abrabla, by adding a γ de-excitation model that can simulate in detailed way the γ-flow in a given final nucleus.

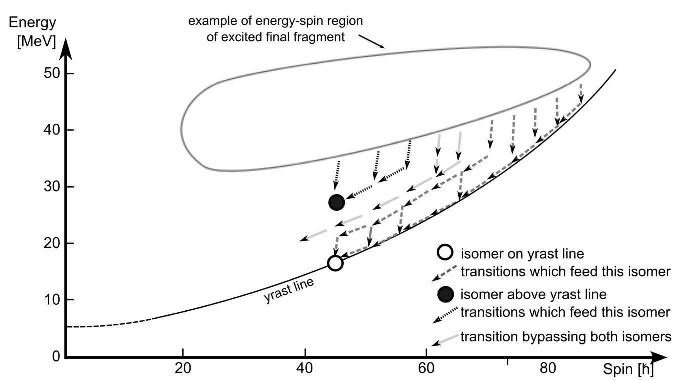

Fig. 2. A schematic drawing showing the possible paths of the γ de-excitation from the entry region of the fragment.

4. Conclusion

The experimental isomeric ratios, both from the present experiment of the relativistic beam fragmentation and from other experiments of this type, were compared with the predictions of 3 models. The results are almost always lower than the theoretical predictions. A possible reason for such a deficit is a lack in the theoretical models of the detailed γ de-excitation path, which will account for the missing γ transitions by-passing the isomer. Additional experiments for other mass regions, and a model in which the γ-decay is properly included, would help us to understand fully the mechanism of population of isomeric states.

This work is supported by research project N-N202-240637 and 1-P03B-030-30 of the Polish Ministry of Science and Higher Education, EURONS (EU contract number 506065). We acknowledge financial support from the UK STFC and AWE plc.

REFERENCES

[1] S. Pietri *et al.*, *Nucl. Instrum. Methods* **B261**, 1079 (2007).
[2] P.H. Regan *et al.*, *Nucl. Phys.* **A787**, 491 (2007).
[3] Zs. Podolyak *et al.*, *Phys. Lett.* **B632**, 203 (2006).
[4] S. Myalski, Ph.D. thesis (2011), unpublished.
[5] S. Myalski *et al.*, *Acta Phys. Pol. B* **40**, 879 (2009).
[6] K.A. Gladnishki *et al.*, *Phys. Rev.* **C69**, 024617 (2004).
[7] M. Pfützner *et al.*, *Phys. Lett.* **B444**, 32 (1998).
[8] M. Pfützner *et al.*, *Phys. Rev.* **C65**, 064604 (2002).
[9] S. Steer *et al.*, *Phys. Rev.* **C84**, 044313 (2011).
[10] M.de Jong *et al.*, *Nucl. Phys.* **A613**, 435 (1997).
[11] J.-J. Gaimard, K.-H. Schmidt, *Nucl. Phys.* **A531**, 709 (1991).
[12] A. Boudard *et al.*, *Phys. Rev.* **C66**, 044615 (2002).
[13] R.J. Charity *et al.*, *Nucl. Phys.* **A476**, 516 (1988).